ISSN 2394-3777 (Print)
ISSN 2394-3785 (Online)
Available online at www.ijartet.com
International Journal of Advanced Research Trends in Engineering and Technology (IJARTET)
Vol. 3, Special Issue 2, March 2016

Molecular structure, spectroscopic (FT-IR and FT-Raman) of 3-butyl-2,6-di (naphthalen-1-yl) phenylpiperidin-4-one: A experimental and DFT study

K.Anandhy[a,b], M. Arockiadoss[c], S. Savithiri[c], G. Rajarajan*[c],S.Mahalakshmi[a]

[a]Post Graduate and Research, Department of Chemistry, Pachaiyappa's College,Chennai-600 030, India.
[b] PG Department of Chemistry, Periyar Govt. Arts College, Cuddalore-607001, India.
[c]Department of chemistry, Annamalai University, Annamalainagar 608 002, India.

Abstract

The structural and spectroscopic analyses of 3-butyl-2,6-di(naphthalen-1-yl) phenylpiperidin-4-one (**3-BDP**) were made by using B3LYP level with 6-31G(d,p) basis set. The optimized parameters showed that the piperidin-4-one ring adopts chair conformation. The B3LYP infrared and Raman spectra were also computed for the **3-BDP** and compared with the experimental spectra.The calculated HOMO and LUMO energies revealed that charge transferthatoccurs within themolecule and Mulliken charges were also obtained. Molecular electrostatic potential (MEP) analyseswere performed to predict the reactive sites of the molecule. The electrical dipole moment (μ) and first hyperpolarizability (βo) values have been computed using DFT/B3LYP-6-31G(d,p) method. The calculated result (βo) shows that the title molecule might have nonlinear optical (NLO) behavior.

Keywords:FT-IR, FT-Raman, hyperpolarizability, HOMO –LUMO.

***Corresponding author:** E-mail: rajarajang70@gmail.com

1. Introduction

Piperidin-4-ones and its derivatives are ubiquitous building blocks in medicinal chemistryand biologically important compounds including the antitumor, antibacterial, antiviral, antimalarial and antiprotozoal activities [1-4]. As well as, such compounds have drawn the concentration of photoscientists because of their huge potential in non- linear optical fields [4,5]. Therefore, the biological importance of piperidin-4-one and its derivatives have strongly stimulated the investigation of computational properties available for these compounds.DFT calculations give accurate results on systems such as large organic molecules[6].Following studies on 3-pentyl-2,6-diphenylpiperidin-4-one [7], 3-pentyl-2,6-di(furan-2- yl)piperidin-4-one [8], we thought to incorporation of napthyl group at 2,6-position of piperidine ring and to extend the study to 3-butyl-2, 6-di (naphthalene-1-yl) phenylpiperidin-4-onewith the aim of characterizing them from the FT- IR and FT-Ramanspectra and to study their quantum chemical descriptor in gas phase by means of a computational approach.In the present study, DFT/ 6-31G (d,p) level theory was used to determine the optimized geometry, vibrational wavenumbers in the ground state, non-linear optical properties, HOMO–LUMO energies and Mulliken charges of the molecules.

ISSN 2394-3777 (Print)
ISSN 2394-3785 (Online)
Available online at www.ijartet.com
International Journal of Advanced Research Trends in Engineering and Technology (IJARTET)
Vol. 3, Special Issue 2, March 2016

2. EXPERIMENTAL

2.1 Synthesis of 3-butyl-2,6-di(naphthalen-1-yl)phenylpiperidin-4-one

3-butyl-2,6-di(naphthalen-1-yl)phenylpiperidin-4-onewas prepared according to the procedure given in literature with a little modification [9]. Dry ammonium acetate (0.05 mol) was dissolved in 50 mL ethanol and the solution was mixed with 1-napthaldehyde (0.1mol) and 2-heptanone (0.05mol) to give a homogenous mixture. Then, the mixture was heated to boiling for about 30 minutes. After cooling, the viscous liquid was dissolved in ether (300 mL) and shaken with 10 mL concentrated hydrochloric acid and the hydrochloride of 3-butyl-2,6-di(naphthalen-1-yl)phenylpiperidin-4-one obtained was separated by filtration and washed with a mixture of ethanol and ether (1:1) to remove most of the coloured impurities. The product was liberated from an alcoholic solution by adding aqueous ammonia and then diluted with water. The crude sample was recrystalized from ethanol. Yield 85%; m.p.: 138-140 (ºC); MF: $C_{40}H_{37}NO_2$; Elemental analysis: Calcd (%): C, 85.22; H, 6.62; N, 2.48; Found (%):C, 84.32; H, 6.50; N, 2.37; IR (KBr) (cm^{-1}): 3466 (N-H stretching), 2956 (ArC-H stretching), 2928Ali.C-H stretching), 1716(C=O stretching), 1437 (C=C stretching), 746 (Aromatic C-H out of plane bending vibration), 590 (Aromatic C-C out of plane bending vibration).

2.2 Spectral measurements

The FT-IR spectrum of the synthesized **3-BDP** was taken in the range 4000-400 cm^{-1} on an AVATAR-330 FT-IR spectrometer (Thermo Nicolet) using KBr (pellet form). The FT-Raman spectral measurements were run from Sophisticated Analytical Instrument Facility (SAIF), Indian Institute of Technology (IIT), Chennai.

2.3 Theoretical background

All calculations were carried out by Density Functional Theory (DFT) on a personal computer using Gaussian 03W program package [10].The calculations were done with the B3LYP level and the basis set 6-31G(d,p) was used in the present study to investigate the molecular and vibrational frequency of molecules in the ground state in order to support and explain the experimental observations. Mulliken, frontier molecular orbital and Non-linear optics (NLO) were calculated from optimized geometry of the molecule.

3. RESULTS AND DISCUSSION

3.1 Geometry Optimization

The optimized bond lengths, bond and dihedral angles of **3-BDP**were calculated by B3LYP method with 6-31G (d,p) basis set level theory and the results are listed in Table 1, in accordance with optimized structure as shown in Fig.1.

ISSN 2394-3777 (Print)
ISSN 2394-3785 (Online)
Available online at www.ijartet.com
International Journal of Advanced Research Trends in Engineering and Technology (IJARTET)
Vol. 3, Special Issue 2, March 2016

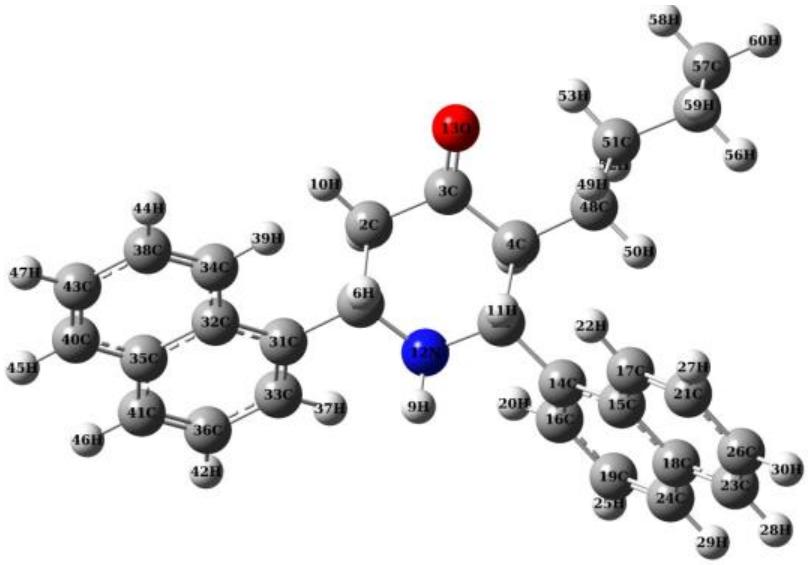

Fig.2. Optimized structures of **3-BDP**

It is found that some of the calculated parameters slightly deviate from experimental values, due to the fact that theoretical calculations belong to the molecule in the gaseous phase, while the experimental results belong to molecules in the solid state. The optimized C3=O13 bond length is calculated as 1.218 Å by B3LYP. This value well matches with the experimental value of 1.211 Å. As seen in Table 1, the calculated bond length N12–H9 is 1.017 (B3LYP) Å which differs from the experimental value by 0.406 Å. This difference is due to the reality that the experimental result corresponds to the intermolecular coulombic interaction with the neighbouring molecules in the solid state [11-13].

Table 1

Selected bond lengths, bond angles and dihedral angles of **3-BDP**.

Bond length (Å)	DFT	XRD[a]	Dihedral(°)	DFT	XRD[a]
N12-H9	1.317	0.911	N12-C5-C4-C48	-179.2	-178.0
N1-C5	1.473	1.471	C2-C3-C4-C48	179.8	177.8
C5-C4	1.568	1.549	C48-C4-C3-O13	-3.6	-7.7
C4-C3	1.530	1.526	H8-C4-C3-O13	-124.4	-
C4-C2	1.518	1.506	N12-C5-C4-C3	55.3	54.8
C2-C1	1.550	1.532	N12-C1-C2-C3	-54.7	-51.9
C3-O13	1.218	1.211			
Bond angle (°)					
C4-C5-N12	108.70	109.32			
C2-C1-N12	107.67	107.47			
C4-C3-O13	123.00	122.01			
C2-C3- O13	121.82	121.93			
C2-C3-C4	115.05	116.06			

a- Values are taken from Ref. [14]

The optimized geometrical parameters are compared with the crystal structure of *t*-3-pentyl-*r*-2,*c*-6-diphenylpiperidin-4-one [14]. It is known from previous studies [15-18] and results from Table 1 that the piperidone ring essentially adopts chair conformation and also it is evident from the torsional angles N12-C1-C2-C3 (-54.7° and -51.9° at B3LYP and XRD, respectively) and N12-C5-C4-C3 [53.3° (B3LYP) and 54.8° (XRD)].The equatorial

ISSN 2394-3777 (Print)
ISSN 2394-3785 (Online)
Available online at www.ijartet.com
International Journal of Advanced Research Trends in Engineering and Technology (IJARTET)
Vol. 3, Special Issue 2, March 2016

orientation of alkyl and aryl groups are identified by their important angles N12-C5-C4-C48 [-179.2 (B3LYP) and -178.0° (XRD)] and C2-C3-C4-C48 [179.8° (B3LYP) and 177.8° (XRD)].

3.2. Vibrational analysis

The FT-IR and FT-Raman spectra of **3-BDP** are shown in Figs. 2a&2b and 2c&2d, respectively. The observed and calculated frequencies by B3LYP level using 6-31G(d,p) basis set along with their relative intensities, probable assignments and potal energy distribution (PED) of the compound are summarized in Table 2 .

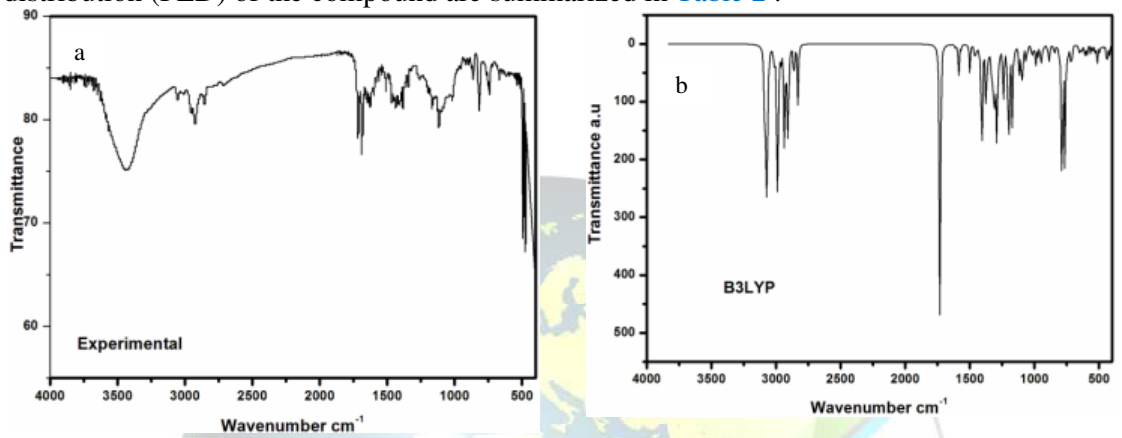

Figs 2 (a)Experimental FT-IR and (b) calculated IR spectra of **3-BDP**

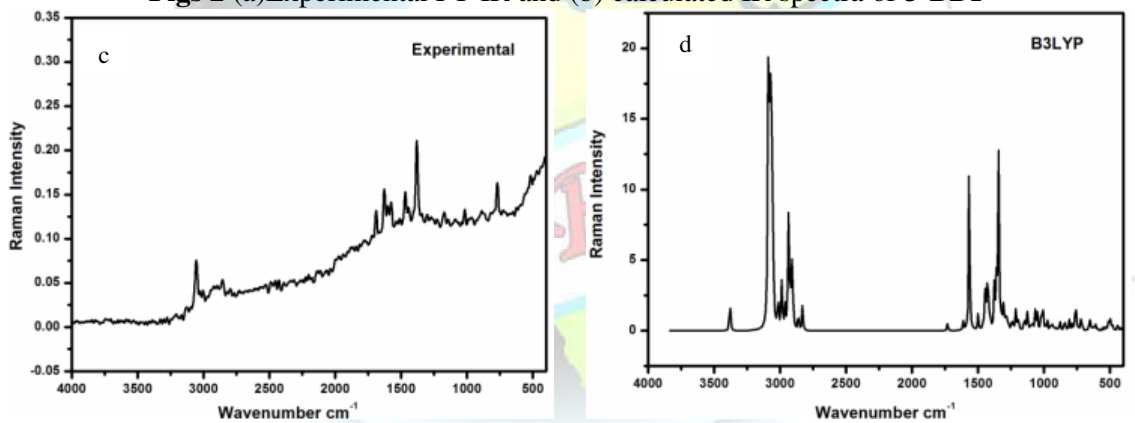

Figs 2 (c) Experimental FT-Raman and (d) calculated Raman spectra of **3-BDP**

The calculated frequencies are scaled by 0.9608 for DFT [8].It is stated that in amines, the N–H [19] stretching vibrations occur in the region 3500–3300 cm^{-1}. With the above reference, the vibrational frequency observed at 3446 cm^{-1} in the infrared spectrum is assigned to the N- H stretching mode, the corresponding computed value matches at 3380 3509 cm^{-1} by B3LYP. The PED corresponding to this vibration contributes to about 100%.In **3-BDP** the C-H stretching vibrations appeared in the range 3063- 3054cm^{-1} B3LYP. The observed frequencies showed at 3058 (FT-IR) and 3054cm^{-1} (FT-Raman) for C-H stretching vibrations. These C-H Stretching vibrations are well supported by PED values.

ISSN 2394-3777 (Print)
ISSN 2394-3785 (Online)
Available online at www.ijartet.com
International Journal of Advanced Research Trends in Engineering and Technology (IJARTET)
Vol. 3, Special Issue 2, March 2016

Table 2 Observed and calculated wavenumbers (cm^{-1}) and PED assignment for 3-BDP.

S No	Experimental		Frequencies		IR intensity	Raman activity	Vibrational Assignments[b] PED≥10%[c]
	FT-IR	FT-Raman	Unscaled	scaled[a]			
1	1015	1016	1059	1018	1.55	4.58	ν N12-C1(25)
2			1150	1105	10.42	3.53	ν C21-C26(29)+ ν C43-C38(22)
3	1116	1117	1165	1119	13.63	4.81	τ C57-C54-C51-C48(10)
4	1170	1173	1222	1175	45.51	1.01	β H52-C51-C54(11)+τ H8-C4-C3-C2(15)
5			1297	1246	1.27	7.33	β H55-C54-C57(14)+τ H56-C54-C51-C48(10)
6	1261		1316	1265	9.08	12.44	β H52-C51-C54(14)+τ H6-C1-C31-C32(10)+ τ H11-C5-C14-C15(20)
7	1342		1399	1344	0.85	59.77	ν C26-C23(11)+rH50-C48-H49(71)
8			1433	1376	12.78	61.72	rH53-C51-H52(16)
9	1380	1381	1445	1388	2.67	2.32	ρ H6-C1-C31(11)
10	1437		1498	1440	1.06	18.29	ρ H50-C48-H49(71)+ ρ H53-C51-H52(16)
11			1503	1444	0.21	12.51	β H42-C36-C41(10)
12		1469	1523	1463	4.75	4.17	ρ H56-C54-H55(18)+ ρ H59-C57-H58(35)+ ρ H60-C57-H59(27)+τ H59-C57-C54-C51(10)
13			1562	1501	6.98	10.31	ν C43-C38(20)
14	1506		1563	1510	9.46	12.94	ν C16-C19(10)+ν C21-C26(19)
15		1576	1643	1579	2.06	133.54	ν C31-C33(11)+ν C33-C36(12)+ ν C32-C35(13)
16	1597		1644	1580	8.60	0.93	ν C19-C24(24)+ν C26-C23(11)+ ν C14-C16(15)
17			1653	1588	9.42	1.77	ν C36-C41(18)+ ν C40-C43(10)+ ν C31-C33(12)
18	1629	1627	1758	1630	1.26	1.41	ν C17-C21(14)+ν C26-C23(13)
19		1689	1759	1690	0.34	9.91	ν O13-C3(20) +ν C21-C26(19)

ISSN 2394-3777 (Print)
ISSN 2394-3785 (Online)
Available online at www.ijartet.com
International Journal of Advanced Research Trends in Engineering and Technology (IJARTET)
Vol. 3, Special Issue 2, March 2016

20	1716		1802	1720	172.75	11.51	ν O13-C3(90)
21	2855	2855	2978	2861	25.56	39.28	ν C5-H11(97)
22			3017	2899	14.80	26.59	ν C51-H52(50)+ ν C54-H55(19)+ ν C54-H56(25)
23	2928	2927	3054	2934	25.83	80.96	ν C48-H49(37)+ν C48-H50(58)
24			3057	2937	26.23	130.20	ν C54-H55(66)+ ν C54-H56(23)
25			3061	2941	9.54	47.13	ν C2-H10(16)+ ν C2-H7(82)
26	2959		3083	2962	6.67	40.56	ν C48-H49(20)+ν C51-H53(62)
27		3054	3179	3054	2.29	82.10	ν C19-H25(22)+ ν C23-H28(17)+ ν C24-H29(43)+ ν C26-H30(10)
28	3058		3188	3063	8.81	134.58	ν C21-H27(65)+ ν C23-H28(21)
29	3446		3517	3380	0.19	79.70	νN12-H9(100)

a- scale factor:0.9608- B3LYP/6-31G(d,p)
b- ν: stretching; β-in-plane bending: ρ- scissoring: r-rocking: Γ- out-of-plane bending: ω- wagging; t- twisting: τ- torsion:
c- PED: Potential energy distribution.

ISSN 2394-3777 (Print)
ISSN 2394-3785 (Online)
Available online at www.ijartet.com
International Journal of Advanced Research Trends in Engineering and Technology (IJARTET)
Vol. 3, Special Issue 2, March 2016

The C-H stretching in alkanes occurs at lower frequencies than those of aromatic ring (3150–3050 cm^{-1}). The CH_3 stretching is expected at 2980–2870 cm^{-1}[20] and usually the bands are weak. Methyl group symmetric stretching appeared at 2959, 2928, 2855cm^{-1} in FT-IR and at 2957 and 2885 cm^{-1} as in FT- Raman spectrum are in agreement with the theoretical value in the range 2962-2861cm^{-1} by B3LYP/6-31 G(d,p) method and it has considerable PED (97-16%) value. The carbonyl group (>C=O) stretching is most important in the vibration spectrum because of its strong intensity absorption [21]. Savithiri*et al*. [22] assigned C=O stretching in the region of 1716cm^{-1} in 3-pentyl-2,6-diphenylpiperidi n-4-one picrate . In this case, the carbonyl C=O stretching appeared at 1716cm^{-1} (FT-IR) and 1689cm^{-1} (FT-Raman). The gas phase value 1720cm^{-1} is in line with experimental values. The PED analysis shows a 90% contribution. The experimental vibration bands at 1437, 1380 cm^{-1} (FT-IR) and 1469, 1381 cm^{-1} (FT-Raman) is assigned to $–CH_2–$ scissoring mode. The theoretically observed value ranges from 1463–1388 cm^{-1}. The rocking mode of $–CH_2–$ is observed in FT- IR at 1342 cm^{-1} and its corresponding theoretical value is 1344cm^{-1} byB3LYP. It has considerable PED values.

3.3. Mulliken Charge Analysis

Mulliken atomic charge calculation plays an important role in the application of quantum chemical calculation to molecular systems[23]. The parameters like dipole moment, polarizability, reactivity depend on the atomic charges of the molecular systems. Table 3display the Mulliken atomic charges of **3-BDP** at the B3LYP/6-31G (d,p) level of theory.The more positive value on C3 atom of C=O group leads to a redistribution of electron density. Some of the carbon atoms C1, C2, C3, C14, C15, C31, C32, C48 and C51 carry the positive charge. Results in Table 3, reveal that the atomic charge of O13and N12carries the larger negative atomic charge. Hence, the hydrogen H8 and oxygen O13 may be the possible reactive sites of **3-BDP**.

Table 3 Mulliken charges of **3-BDP**

Atom	Charge	Atom	Charge
C1	0.1110	C26	-0.0001
C2	0.0368	C31	0.0317
C3	0.4078	C32	0.0740
C4	-0.0051	C33	-0.0331
C5	0.0993	C34	-0.0444
N12	-0.2978	C35	0.0993
O13	-0.4529	C36	-0.0064
C14	0.0263	C38	-0.0075
C15	0.0671	C40	-0.0466
C16	-0.0204	C41	-0.0411
C17	-0.0405	C43	-0.0005
C18	0.1007	C48	0.0386
C19	-0.0046	C51	0.0112
C21	-0.0075	C54	-0.0007
C23	-0.0466	C57	-0.0067

ISSN 2394-3777 (Print)
ISSN 2394-3785 (Online)
Available online at www.ijartet.com
International Journal of Advanced Research Trends in Engineering and Technology (IJARTET)
Vol. 3, Special Issue 2, March 2016

C24	-0.0414		

3.4. Molecular electrostatic potential (MEP)analysis

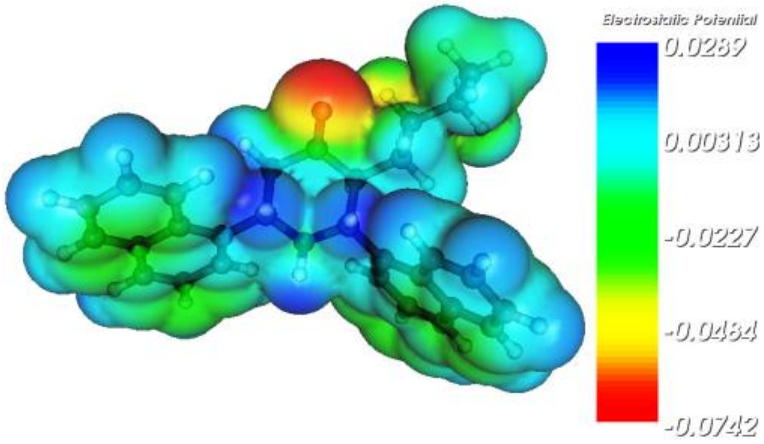

Fig 3 MEP surface diagram of **3-BDP**

To predict reactive sites of electrophilic and nucleophilic attacks for the investigated molecule, MEP at the B3LYP/6-31G (d,p) optimized geometry is calculated. The negative (red and yellow) regions of MEP are associated with electrophilic reactivity and the positive (blue) regions to nucleophilic reactivity (Fig. 3).As seen in Fig. 3, negative regions, where come into existence nucleophilic attack, are oxygen atoms in C=O moiety. Conversely, the regions having positive potential where an electrophilic attack to molecule happens are H9 and benzene ring.

3.5. *Frontier molecular orbital analysis*

A deeper understanding of chemical reactivity will be gained by the electronic absorption which corresponds to the transition from the ground to the first excited state and it is mainly represented by one electron excitation from the highest occupied molecular orbital (HOMO) to the lowest unoccupied molecular orbital (LUMO) [23]. The HOMO represents the ability to donate an electron and LUMO represents the ability to gain an electron. So as to evaluate the energetic behavior of the title compound, we make calculations in gas phase, ethanol and chloroform solvents. 3D plots of the HOMO and LUMO orbitals computed at the TD-B3LYP/6-31G(d, p) level of **3-BDP** molecule, in the gas phase, are illustrated in Fig. 4.It is clear from the figure that the HOMO is located mainly over the entirenapthyl and piperidine ring. The napthyl ring and carbonyl group oxygen covered in LUMO values.

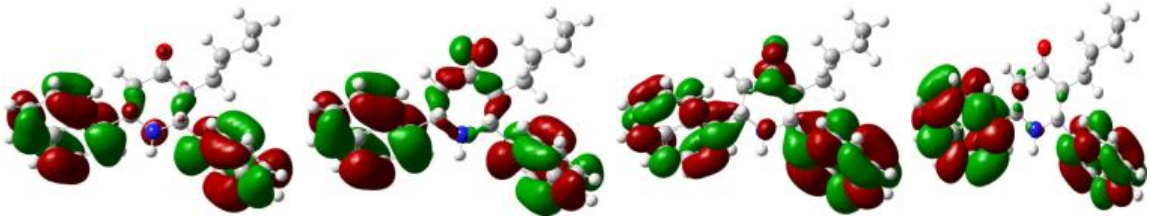

HOMO-1 HOMO LUMO LUMO+1

Fig. 4 Molecular orbitals and energies for the HOMO and LUMO in gas phase

ISSN 2394-3777 (Print)
ISSN 2394-3785 (Online)
Available online at www.ijartet.com
International Journal of Advanced Research Trends in Engineering and Technology (IJARTET)
Vol. 3, Special Issue 2, March 2016

The calculated energy values of HOMO are -5.79, -5.72, and -5.73eV in gas, ethanol and chloroform, respectively. LUMO is -1.21, -1.13, and -1.14 eV in gas, ethanol and chloroform, respectively. The value of the energy separation between HOMO and LUMO is 4.58, 4.59 and 4.59 eV in gas, ethanol and chloroform, respectively. The energy gap of HOMO-LUMO explains the eventual charge transfer interaction taking place within the molecule, which influences the biological activity of the molecule. Furthermore, in going from the solution to the gas phase, an increasing value of the energy gap shows that the molecule becomes more stable.

The absolute electronegativity (χ), hardness (η), electrophilicity index (ψ) and softness (ζ) are calculated using the following equations

$\eta = (IP-EA)/2 \approx (E_{LUMO}-E_{HOMO})/2$

$\chi = (IP+EA)/2 \approx -(E_{LUMO}+E_{HOMO})/2$

$\psi = \mu^2/2\,\eta$

$\zeta = 1/2\,\eta$

Table4 Calculated energy values of **3-BDP** in gas phase, ethanol and chloroform.

DFT/B3LYP/6-311G(d,p)	Gas	C_2H_5OH	CH_3Cl
E_{HOMO}	-5.79	-5.72	-5.73
E_{LUOMO}	-1.21	-1.13	-1.14
$E_{LUMO-HOMO}$	4.58	4.59	4.59
E_{HOMO-1}	-5.90	-5.81	-5.83
$E_{LUOMO+1}$	-1.11	-1.02	-1.04
$E_{(LUMO+1)-(HOMO-1)}$	4.79	4.79	4.79
Electrinegativity(χ)	-3.50	-3.42	-3.44
Hardness(η)	2.29	2.29	2.29
Electrophilicity index(ψ)	2.68	2.56	2.57
softness(s)	161.62	161.43	161.38
Dipolemoment (Debye)	2.74	3.68	3.43

For **3-BDP**, electronegativity (χ), hardness (η), electrophilicity index (ψ) and softness (ζ) are given in Table 4. The dipole moment is another important electronic property in a molecule. For example higher the dipole moment, the stronger will be the intermolecular interactions. The calculated dipole moment values are given in Table 4. Based on predicted dipole moment values, it is found that, in going to the solvent phase from (6.68 D in ethanol) from gas phase (4.74 D), the dipole moment value decreases thatindicates thepolarity of solvent influences the dipole moment of the studied molecule.

3.6. Non-linear optical activity

NLO is important property providing key for areas such as telecommunications, signal processing and optical interactions [12,22]. A large variety of NLO switches exhibiting large changes in the first order hyperpolarizability (β_0), the molecular second-order NLO response.The calculated and first-order molecular hyperpolarizability (β) and dipolemoment (μ) of the compound are 0.76 x 10-30 esu and 2.74 D, respectively [Table 5].

ISSN 2394-3777 (Print)
ISSN 2394-3785 (Online)
Available online at www.ijartet.com
International Journal of Advanced Research Trends in Engineering and Technology (IJARTET)
Vol. 3, Special Issue 2, March 2016

Table 5 Some molecular properties of **3-BDP** calculated using B3LYP/6-31G (d,p) level theory in gas phase.

Parameter	Dipolemoment	Parameter	Hyperpolarisability
μ_x	-0.2996	β_{xxx}	-67.8952
μ_y	-2.7218	β_{yyy}	-34.119
μ_z	-0.1608	β_{zzz}	4.8597
μ_{total} (D)	2.743	β_{xyy}	19.8443
	Polarisability	β_{xxy}	-45.854
α_{xx}	166.95	β_{xxz}	33.6522
α_{yy}	188.82	β_{xzz}	9.8093
α_{zz}	172.62	β_{yzz}	1.3549
α_{xy}	-4.38	β_{yyz}	-24.688
α_{xz}	0.62	β_{xyz}	-22.781
α_{yz}	4.06	β_0 (esu)	0.765×10^{-30}
α_o (esu)	2.61×10^{-23}		
$\Delta\alpha$ (esu)	2.44×10^{-24}		

As we compare the hyperpolarizability (β_0) of compound **1** with urea [24], the value is 2 times greater than that of urea. High β_0 value is a required property of a NLO material. It is possible to sustain nonlinearity at the macro level by crystal designing using proper substituents. Therefore, the title compound has a potential use in the development of non-linear optical materials.

6. Conclusions

A comparison of calculated and experimental geometrical parameters shows that the piperidin-4-one ring adopts chair conformation. The FT-IR and FT-Raman spectra were also well reproduced by the B3LYP calculation.In addition, Mulliken charge analysis and MEP predictthe most reactive parts in the molecule.The calculatedHOMO and LUMO energies were used to analyze the charge transferwithin the molecule.The calculated dipolemoment and first order hyperpolarizability results indicate that the molecule has a reasonablygood nonlinear optical behaviour.

Reference

[1] D.L. Klayman, J.F. Bartosevich, T. Scott Griffin, C.J. Mason, J.P. Scovill, J. Med. Chem., 22 (1979) 855-862.
[3] M. Gopalakrishnan, P. Sureshkumar, J. Thanusu, V. Kanagarajan, J. Korean Chem. Soc., 52 (2008) 503-510.
[3] N. Bharti, K. Husain, M.T. Gonzalez Garza, D.E. Cruz-Vega, J. Catro-Garza, B.D. Mata-Cardenas, F. Naqvi, A. Azam, Bioorg. Med. Chem. Lett., 12 (2002) 3475-3478.
[4] J. Jayabharathi, V. Thanikachalam, M. Padamavathy, N. Srinivasan, Spectrochim. Acta Part A 81 (2011) 380-389.
[5] J. Jayabharathi, V. Thanikachalam, M. Padamavathy, M. VenkateshPerumal, J. Fluoresc., 22 (2012) 269-279.
[6] C. Lee, W. Yang, R. G. Parr, Phys. Rev. B 37 (1988) 785 -789.
[7] S. Subashchandrabose , H. Saleem, Y. Erdogdu , G. Rajarajan , V. Thanikachalam, SpectrochimicaActa Part A 82 (2011) 260-269.

[8] M. Arockia doss, S. Savithiri, G. Rajarajan, V. Thanikachalam, C. Anbuselvan, SpectrochimicaActa Part A 151 (2015) 773–784.
[9] M. Arockia doss, S. Savithiri, S. Vembu, G. Rajarajan, V. Thanikachalam, Can. Chem. Trans., 2 (2015) 261-274.
[10] M.J. Frisch, et al., Gaussian 03, Revision E.01, Gaussian Inc, Wallingford, CT,2004.
[11] R.M.S. Alvareza, M.I.M. Valdeza, E.H. Cutin, C.O.D. Vedova, J. Mol. Struct., 657 (2003) 291–300.
[12] M. Arockia doss, S. Savithiri, G. Rajarajan, V. Thanikachalam, H. Saleem, SpectrochimicaActa Part A 148 (2015) 189-202.
[13] M.E. Tuttolomondo, P.E. Arganaraz, E.L. Varentti, S.A. Hayes, D.A. Wann, H.E. Robertson, D.W.H. Rankin, A.B. Altabef, Eur. J. Inorg. Chem., 10 (2007) 1381– 1389.
[14] P. Gayathri, J. Jayabharathi, G. Rajarajan, A. Thiruvalluvar, R.J. Butcher, ActaCrystallogr., 65E (2009) o3083.
[15] S. Savithiri, G. Rajarajan, V. Srividhya, J. Jijesh, V. Thanikachalam, J. Jayabharathi, M. Arockiadoss, Can. Chem. Trans., 2(2014) 201-220.
[16] S. Savithiri, M. Arockia doss, G. Rajarajan, V. Thanikachalam, Can. Chem. Trans.,2 (2014) 403-417.
[17] S. Savithiri, M. Arockia doss, G. Rajarajan, V. Thanikachalam, S. Bharanidharan, H. Saleem, SpectrochimicaActa Part A 136 (2015) 782–792.
[18] S. Savithiri, M. Arockia doss, G. Rajarajan, V. Thanikachalam, J. Mol. Struct., 1075 (2014) 430–441.
[19] D.L. Pavia, G.M. Lampman, G.S. Kriz, J.R. Vyvyan, Spectroscpoy, CengageLearing, New York, 2008.
[20] G. Socrates, Infrared Characteristic Group Frequencies, John Wiley and sons, New York, 1980.
[21] R.M. Silverstein, F.X. Webster, Spectroscopic Identification of Organic Compounds, 7th(Edn), Wiley, New York, 2005.
[22] S. Savithiri, M. Arockia doss, G. Rajarajan, V. ThanikachalamJ. Mol. Struct., 1105 (2016) 225-237.
[23] K. Gokula Krishnan, R. Sivakumar, V. Thanikachalam, H. Saleem, M. Arockia doss, SpectrochimicaActa Part A 144 (2015) 29–42.
[24] Z.-M. Jin, B. Zhao, W. Zhou, Z. Jin, Powder Diff. J. 12 (1997) 47-48.